SolarPACES 2022, 28th International Conference on Concentrating Solar Power and Chemical Energy Systems
Receivers and Heat Transfer Media and Transport: Linear Systems
https://doi.org/10.52825/solarpaces.v1i.659

Published: 05 Jan. 2024

Linear Beam-Down Solar Field Demonstrator: First Results and Validation

S. Taramona[1][https://orcid.org/0000-0002-7179-1941], A. Gallo[1,2][https://orcid.org/0000-0001-8157-2278], E. LaTourrette-Ghez[3][https://orcid.org/0000-0003-1434-5002], J. Gómez-Hernández[1][https://orcid.org/0000-0001-8053-4368], and J.V. Briongos[1][https://orcid.org/0000-0002-1837-7135]

[1] University Carlos III of Madrid, Spain

[2] University of Almería, Spain

[3] Johns Hopkins University, US

Abstract. Linear beam-down solar fields consist of two stages of reflections that allow to concentrate solar irradiance at ground level. This approach seems promising for coupling with certain industries that require process heat, such as in mining and asphalt industries, in order to reduce their carbon emissions. In this work, the design and construction of a first of its kind linear beam-down Fresnel prototype is presented. First tests show that for the current solar field configuration, concentrations of up to 4.53 suns are achieved for a summer day at around 4 PM local time (UTC +2). Simulation projections show that this result could be enhanced to obtain up to 11.5 suns under the same solar conditions, by improving the mirror aiming system.

Keywords: Concentrated Solar Power, Linear Fresnel Reflectors, Prototype Experiments

1. Introduction

Considering the goal of reducing carbon emissions, Concentrated Solar Power (CSP) is a technology with great potential, as it is not widely implemented and is capable of supplying direct heat to industrial processes where other approaches might be too expensive or complicated. CSP is based in harnessing the heating power of concentrated solar irradiation, this way, using multiple mirrors, the solar heating power is multiplied and can be used for electric power generation or supplying process heat. Linear Fresnel reflectors concentrate solar power using low-curvature long mirrors, redirecting the solar irradiance linearly above the mirror level, parallel to the ground. Including a secondary beam-down reflector has been considered in previous studies, initially using a hyperbolic-cylinder mirror [1], then using several flat mirrors [2]. Incorporating this modification allows the solar field to concentrate the solar irradiance at ground level as displayed in Figure 1, which enables the direct use of the concentrated sun light to heat heavier products, such as aggregates for the asphalt industry or bio-wastes, to temperatures between 150 and 250ºC [3]. A prototype that incorporates this technology has been built, and it is expected to achieve concentrations of up to 11.5 suns throughout the year, which would facilitate the integration of this solar technology into asphalt production industry. This result is lower than the industrial standard [4], but that is expected, since flat mirrors are used and a second reflection stage is added. To measure the solar concentration and distribution that reaches the receiver region, a procedure similar to [5] is used, where a CCD camera and a radiometer are combined to characterize the concentrated spot.

In this communication the first heat flux measurements obtained with the constructed beam-down prototype are presented, as well as the comparison with the expected results from

the simulations, and the necessary measures to fix the aiming and tracking problems encountered during the experimental campaign of this first version of the prototype, understanding aiming as the initial or static tilt of the mirrors to reflect the sunrays to the focal point, and tracking as the constant movement of the mirrors to update their angle according to the movement of the sun.

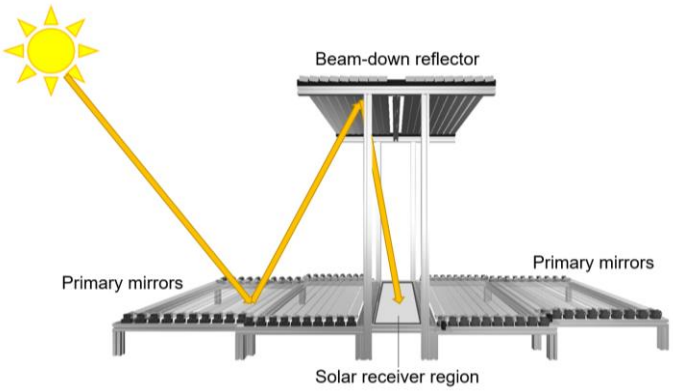

Figure 1. Beam-down linear Fresnel reflector working principle.

2. Solar field

A beam-down linear Fresnel reflector prototype has been designed and constructed, and is displayed in Figure 2. The designed solar field is composed of 3 different stages: the first one is the primary mirror field located near the ground, the second one is the secondary reflector placed above the first stage, and the last stage is the solar receiver, where the solar irradiance is concentrated. The followed philosophy when designing the prototype was to obtain a cheap lab-scale beam-down linear Fresnel reflector, which could be easily constructed and moved around in order to safely store it and take it outside to take solar measurements. The general dimensions of the solar field are displayed in Figure 2-A, while a picture of the prototype in the storage location is presented in Figure 2-B.

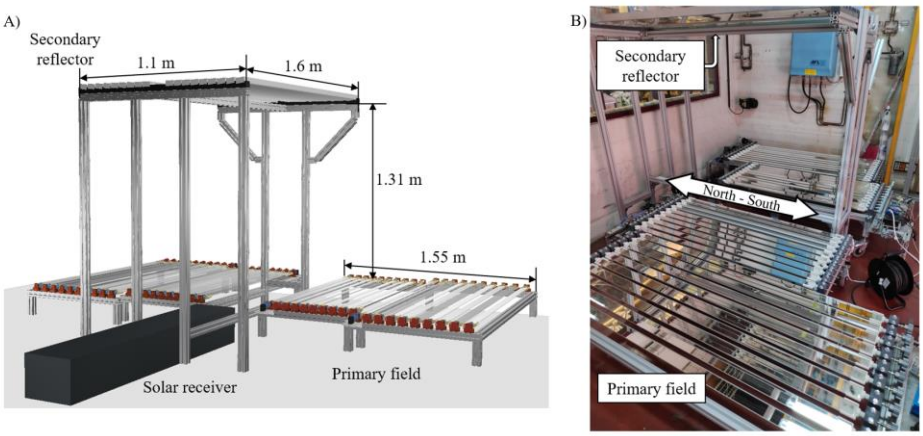

Figure 2. Proposed solar field design and construction. A) Render with dimensions. B) Prototype in the storage room.

2.1 Primary mirrors

The primary field is composed of a total of 40 flat mirrors 5.5 cm wide in order to reduce prototype costs. These mirrors are divided in 4 independent sets of 10 mirrors each, where the two sets closer to the center of the field are 1.35 m long, and the other two are 1.6 m long.

Each set is equipped with a set of wheels to easily move it around and locate it in the desired position.

Every mirror of each set is reinforced with an aluminum T-profile, and properly placed in the design position by anchoring it to the structure with a support system that can be coupled to a tracking device. Since the relative angle between the mirrors is constant, a tracking rack-and-pinion system has been implemented for each set to move the mirrors to the desired angle according to the solar position. This movement is controlled using an Arduino board.

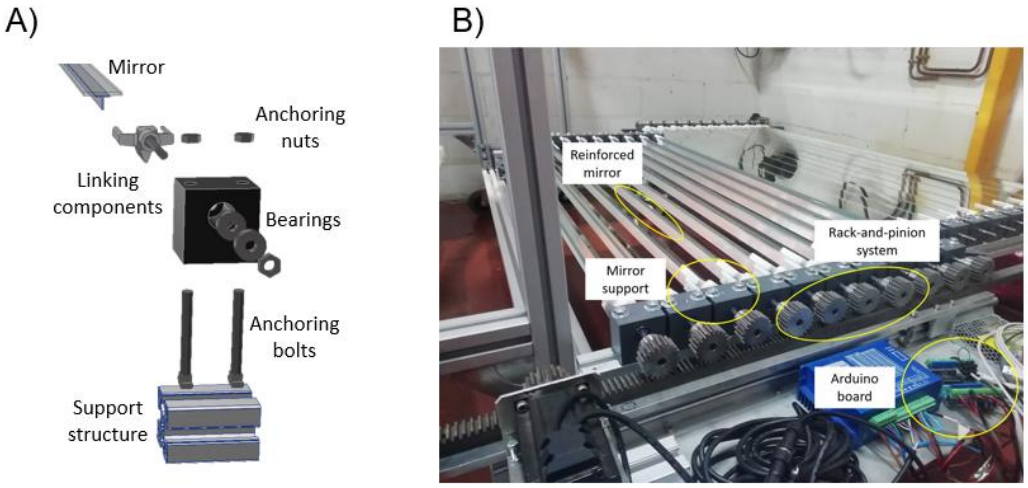

Figure 3. Primary mirror field details. A) Mirror support system and anchoring. B) Prototype result.

In Figure 3 A, the exploded view of anchoring system to the structure is displayed, showing its different components. It can be seen how the mirror and aluminum beam are coupled to the support structure using some bolts and two specially designed linking components. On the other hand, in Figure 3 B, the different components of the primary mirror set are displayed: the reinforced mirrors with their support and anchoring system, the rack-and-pinion system to move the mirrors, and the Arduino board to control the tracking of the mirrors.

The procedure to lock up the mirrors in their proper relative angle goes as follows: once the correct placement of the mirror in the field is obtained, the support system is locked up in a way that maximizes the contact between the rack and the pinion, after that, with the rack blocked, the mirror is tilted to the correct angle and then it is locked up to the pinion by using a special metal cap that connects the pinion to the bolt that acts as support of the mirror and using a nut to block this cap, this way the mirror angle can be fixed to a specific position of the rack.

2.2 Secondary reflector

The beam-down reflector is located 1.31 m above the primary field, and it is composed of 18 fixed mirrors 5 cm wide and 1.6 m long, 9 for each side of the solar field. These mirrors are also reinforced with an aluminum T-profile and are located in the correct position and with the desired angle using a special support to anchor them to the structure. In Figure 4 the design of the secondary reflector, as well as the prototype result are presented.

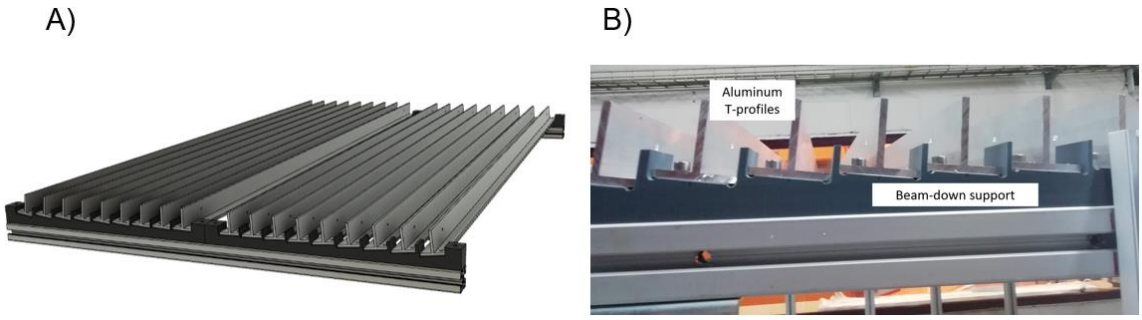

Figure 4. Secondary reflector details. A) Render of the design.
B) Close-up picture of the beam-down prototype.

In Fig. 4 A, the render of the complete beam-down design is displayed, showing how the mirrors are properly located and tilted over the support structure. In Figure 4 B, a close-up picture of the secondary reflector is portrayed, showing how the beam-down support is used to obtain the desired angle of each mirror, and to keep them in their desired position, by anchoring the mirrors using the aluminum beams.

2.3 Solar receiver

For this experiment, the solar receiver consists of a Lambertian target, which diffusely reflects the incident radiation. This target is located at the same height as the primary mirrors and can be moved in two directions parallel to the ground level. It also allows the coupling of the irradiance sensor. This Lambertian target is displayed in Figure 5.

Figure 5. Top view picture of the Lambertian target indicating the location of the sensor.

The target is 35 cm long and 29 cm wide, and the aperture to couple the sensor is located 5.8 cm from the closest edge of the target and in the center of the other axis. This target can be moved in both directions of its plane by turning two different worm screws, one for each direction, as displayed by the arrows in Fig. 5.

3. Methodology

Experimental measurements were taken and compared with SolTrace simulations [6]. These experiments were carried out at Carlos III University of Madrid, in Spain, located 40.33º North and 3.77º West. By using a Hukseflux HFS01 radiometer (thermopile water-cooled sensor) that measures between 0 and 20 kW/m^2, and that is coupled to the Lambertian target displayed in Figure 5, the concentrated heat flux is measured. Additionally, a CCD Basler scA1300-32 gm camera, fixed to the beam-down, is aimed towards the Lambertian target in order to obtain

images with a spatial distribution of the heat flux on the objective. By combining the greyscale values of the images with the radiometer results, the irradiance distribution on the target was estimated in terms of kW/m^2. Two pyranometers, one for measuring the total irradiance (model SR05-D1A3), and another for measuring diffuse irradiance (model SR15-D2A2), are used to obtain the direct irradiance, which combined with the radiometer measurements allows to obtain the total concentration of the solar field. The complete prototype setup, prepared to take measures, is presented in Figure 6, with the mirrors in their correct position, the motors connected to the Arduino board. The solar field is positioned in the desired North-South orientation and each mirror set is located in the correct position to be able to correctly track the sun, and it can be adjusted along its length to maximize the concentration on the receiver.

Figure 6. Solar prototype setup outdoors.

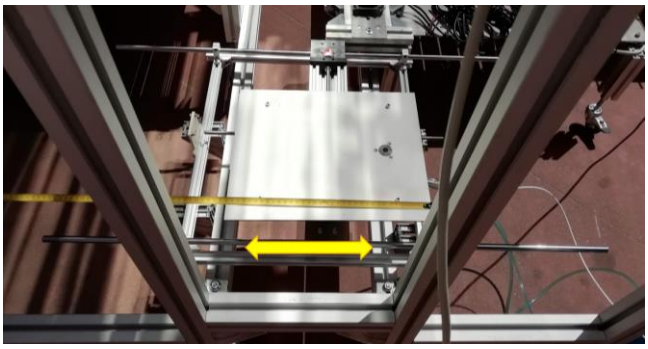

Figure 7. Top view picture of the target with the concentrated solar irradiance. and the direction of the objective's movement.

In Figure 7 a detail of the Lambertian target with the incident concentrated sunrays is depicted. It can be seen how the solar irradiance is concentrated in different sections of the objective, the brighter the section, the higher the concentration.

The experimental procedure started with the orientation of the primary mirrors. Once the measurement time was determined the angle of the mirrors for said time was calculated, and the different mirror sets were set up by adjusting the closest mirror to the midfield for the closest sets, and the furthest mirror for the external sets, to the desired angle. Since all the mirrors move together due to the rack-and-pinion system, all the mirrors should be properly angled. Once the mirrors were tilted, their inclination was measured and the Lambertian target was slowly moved in the direction of the arrow in Figure 7, starting and ending in a similar position, to measure the obtained heat flux and to characterize the concentration profile observed by the CCD camera.

With the measured angles, SolTrace simulations are performed. With these results the simulated irradiance distribution is compared with the experimental one, as well as the heat flux, as it will be observed in the next section, the obtained experimental results were not particularly close to the desired ones. By adjusting the simulation parameters to best match the experimental results, a realistic approximation can be obtained for a more precise version of the prototype, by adjusting the encountered aiming and tracking errors in the current version.

4. Results and discussion

Once the prototype was properly set-up with all the mirrors in the correct positions and with the desired inclination, the Lambertian target in the right location, and all the sensors properly working, we started quantifying the different relevant parameters: the global and diffusive irradiance, the heat flux that reaches the receiver, and the inclination of the mirrors. These measurements were taken on July 18th, 2022 (day number 199 of the year) at 4:06 PM CET. The irradiance results for all sensors are displayed in Figure 8.

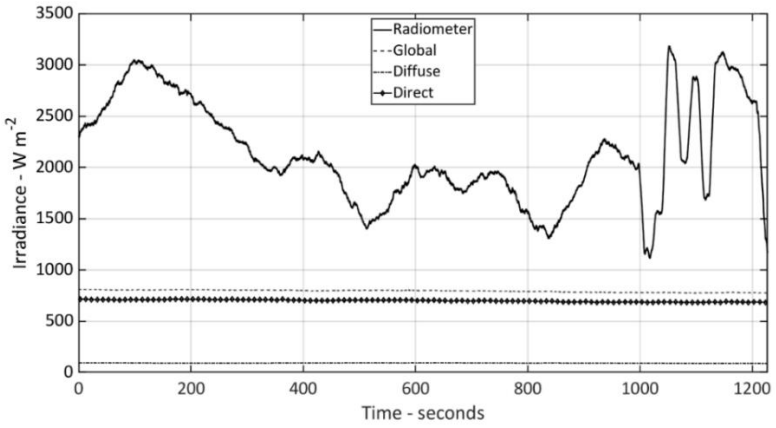

Figure 8. Irradiance measurements for July 18th.

As it can be observed, the total measurement time was 1200 seconds (approximately 20 minutes). The first 1000 seconds were used to set the inclination of the mirrors and measure the angles of all of them, note that once the mirror tilt was set, there was no solar tracking so the position of the mirrors remained fixed while the sun kept moving, hence the fluctuation of the radiometer measures, as it tracked the variation of the concentration profile with the movement of the sun. The solar motion can be noticed in Figure 8 by the slight decrease of the global solar irradiance (from 809 to 778 W/m^2). Near the end of the measuring process, after the 1000 second mark, the radiometer was first located close to the eastern end of the receiver region, in the furthermost brightest spot, and then slowly moved to different positions in the focal range to characterize the CCD camera image, spanning over 7.5 cm and turning back, ending up in a similar position to the one in which the measurement started. The obtained irradiance varied between 1000 and slightly more than 3000 W/m^2. At about 1050 seconds the maximum irradiance recorded was around 3150 W/m^2, which corresponds to a local concentration of approximately 4 suns. However, it is important to note that this is not the maximum irradiance obtained on the receiver. To know the maximum irradiance, it is necessary to calibrate the grayscale images obtained with the CCD camera by applying a linear regression with the radiometer measures.

By measuring the angles of each mirror during the experimental data acquisition process, different SolTrace Monte Carlo Ray-Tracing simulations are executed until the obtained simulated result fits the experimental one, both in maximum and minimum measured heat flux and in the solar concentration profile. Considering a direct irradiation of 695 W/m^2 as obtained from the pyranometers, a reflectivity of 0.81, and a slope and specularity error of 3.15 mrad for the mirrors, a peak heat flux of 3142 W/m^2 and a minimum flux of 1145 W/m^2 are obtained

which matches the range displayed in Figure 8, while an average heat flux of 2069 W/m^2 is achieved over the receiver width. In Figure 9 the concentration profiles of both the simulation and the experiment are displayed side by side, as it can be seen, both are very similar.

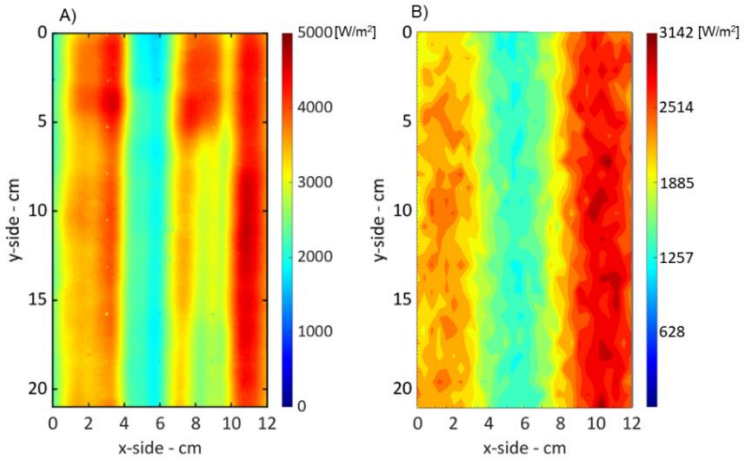

Figure 9. Solar concentration distribution. A) Experimental. B) Simulated.

As it can be seen, the general shape of both distributions is overall similar. However, there are certain discrepancies in both axes. In the longitudinal axis (Y-axis in Figure 9), the main difference is a higher concentration in the upper region of the experimental image, this is because of the distribution of the primary mirrors in the solar field, as some mirrors end up further away from the middle of the target. On the other hand, in the perpendicular X-axis, the discrepancies can be explained because the simulation result is a picture taken at a certain specific time, the experimental results take some time to acquire, and during this time sun keeps moving. These differences can be better appreciated in Figure 10 A, where a blend of both results is displayed, showing the similarities of both profiles, and in Figure 10 B, where a differential plot of both results is portrayed. It is important to note that in this latter plot, the darker the image, the more similar the sources are, so it can be seen in this figure that the main difference is located in the right side of the image, and along its whole length.

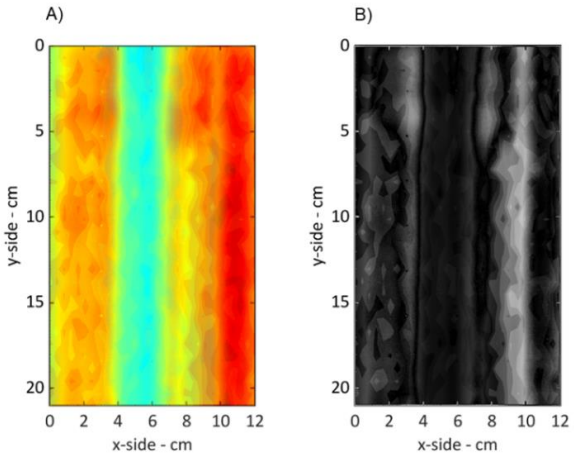

Figure 10. Experimental and simulated results comparison. A) Experimental and simulation blend. B) Differential result between experiment and simulation.

The next interesting result is the potential solar concentration obtainable by improving the prototype conditions. The most important parameter to improve is the relative angle of the

mirrors. Because of the current design, the mirror inclination was defined manually, and was locked by tightening a nut against a custom-made cap. By constantly adjusting and moving the solar field mirrors, this system can be loosened, and the original relative angles are lost. When comparing the ideal angles with the measured ones, an average deviation of 5.24 mrad is obtained, with a maximum error of 64.58 mrad for certain mirrors. By adjusting the mirrors to their correct inclination, a maximum irradiance of 8027 W/m^2 with an average heat flux of 6116 W/m^2 is achieved. This means that the maximum irradiance could increase to 2.55 times, while the average heat flux 2.96 times the current value. As it can be seen in Figure 11, the obtained profile presents a normal distribution, with the highest heat flux in the center of the receiver.

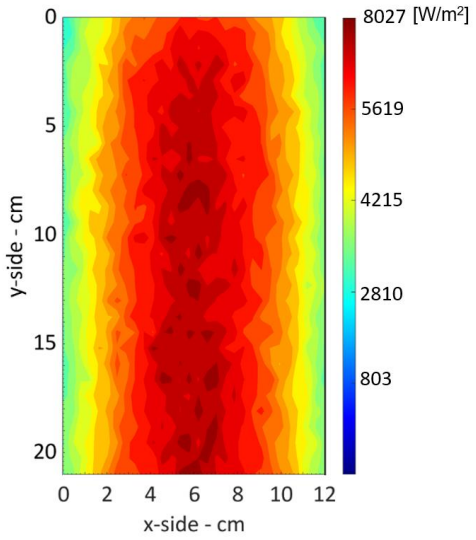

Figure 11. Solar concentration distribution with improved aim.

This result shows the potential of this presented technology: being able to concentrate up to 11.5 suns by using only flat mirrors.

It is evident that the desired result was not obtained in the experimental sessions. This campaign was the first approach to the construction and start-up of this kind of technology, and we encountered many unexpected setbacks and difficulties. The most influential problem was the set-up of the correct mirror tilts, since they are bound together in groups of 10 and their relative angles must be properly fixed in their respective positions. The main issue was fixing all the mirrors to their correct angle while being connected between them through the transmission system, so tightening one of the mirrors might affect the angle between said mirror and the adjacent ones.

The rack-and-pinion tracking system did not end up working with the required precision, and ended up inducing aiming and tracking errors, as it will be seen in the obtained results. With the current system. The main problem was found when tightening multiple nuts to the same rack, as the torque induces slight movements on both, the rack and the mirror, and the system ends up with slight divergences from the desired relative angles.

The second problem comes from the usage of the system itself, as constantly moving the mirrors may induce an untightening of the nuts, and consequently a loss of the relative angles. Additionally, the inherent hysteresis of the system and the clearance between the rack and pinions means that sometimes the mirrors do not move to the desired tilt as determined by the Arduino board. This problem worsens when constantly changing the direction of the rotation.

These problems are the main reason why the concentration profile obtained in the experimental campaign does not match the desired one.

5. Conclusions and future works

A first of its kind beam-down linear Fresnel reflector prototype has been designed and constructed. Experimental measurements have been obtained using this prototype, which have been compared with simulation results, where the maximum heat flux obtained is 3150 W/m^2, which corresponds to a concentration of 4.53 suns, with an average of 2069 W/m^2. Additional simulation results show that this prototype can be theoretically improved to obtain an average concentrated irradiance of 6116 W/m^2 or 8.8 suns, by just improving the aim of the mirrors.

Regarding future works, a new version of the prototype will be developed in order to improve the obtained performance. This includes reducing the number of mirrors and removing the rack-and-pinion tracking system, which will reduce the aiming deviations and allow to obtain the desired relative angles between mirrors. Additionally, a closed system loop will be implemented to constantly check the mirror tilts and improve the aiming and tracking.

Data availability statement

The data obtained in the experimental campaign can be accessed online.

Author contributions

The contribution of the different authors can be distributed as follows:

The conceptualization of the project was organized by S. Taramona, J. Gómez-Hernández and J.V. Briongos. The investigation, software development and visualization was conducted by S. Taramona, A. Gallo and E. LaTourrette-Ghez. The supervision and funding acquisition was obtained by J. Gómez-Hernández and J.V. Briongos, while the original draft was written by S. Taramona, and the review and editing was also done by A. Gallo, J. Gómez-Hernández and J.V. Briongos.

Competing interests

The authors declare no competing interests.

Funding

The research project INTECSOLARIS-CM-UC3M has been funded by the call “Programa de apoyo a la realización de proyectos interdisciplinares de I+D para jóvenes investigadores de la Universidad Carlos III de Madrid 2019-2020” under the frame of the “Convenio Plurianual Comunidad de Madrid - Universidad Carlos III de Madrid”.

The authors wish to thank “Comunidad de Madrid” for its support to the ACES2030-CM Project (S2018/EMT-4319) through the Program of R&D activities between research groups in Technologies 2018, co-financed by European Structural Funds.

The research project SHHIP-CO2 (PID2021-122278OB-I00) has been funded by the call “Proyectos de generación de conocimiento” under the frame of the “Programa Estatal para Impulsar la Investigación Científico-Técnica y su Transferencia”.

Acknowledgements

Special thanks to the lab technicians, who helped make the solar prototype a reality, and to the department colleagues who helped with the solar field setup for the experimental data acquisition.

References

1. A. Sánchez-González, J. Gómez-Hernández, “Beam-down linear Fresnel reflector: BDLFR”. Renewable Energy, vol. 146, pp. 802-815, Feb. 2020, https://doi.org/10.1016/j.renene.2019.07.017.
2. S. Taramona, P.A. González-Gómez, J.V. Briongos, J. Gómez-Hernández, “Designing a flat beam-down linear Fresnel reflector”. Renewable Energy, vol. 187, pp. 484-499, Mar. 2022, https://doi.org/10.1016/j.renene.2022.01.104.
3. D. Pardillos-Pobo, J. Gómez-Hernández, T. Otanizar, “Modelling a conveyor-belt solar receiver to dry and heat aggregates in hot mix asphalt industry”. 2nd Solar Energy Systems Conference, Aug. 2020.
4. M. Babu, S.S. Raj, A. Valan Arasu, “Experimental analysis on Linear Fresnel reflector solar concentrating hot water system with varying width reflectors”. Case Studies in Thermal Engineering, vol. 14, Sep. 2019. https://doi.org/10.1016/j.csite.2019.100444.
5. M.M. Mokhtar, S.A. Meyers, I. Rubalcaba, M. Chiesa, P.R. Armstrong, “A model for improved solar irradiation measurement at low flux”, Solar Energy, vol. 86, pp. 837-844, Mar 2012, https://doi.org/10.1016/j.solener.2011.12.012.
6. T. Wendelin, A. Dobos, A. Lewandowski, “SolTrace: A Ray-Tracing Code for Complex Solar Optical Systems”, NREL, 2013